AGU ADVANCING EARTH AND SPACE SCIENCE

Geophysical Research Letters®

RESEARCH LETTER
10.1029/2022GL099115

Key Points:

- ^{14}C, excess ^{210}Pb, and Bayesian statistics can produce decadal age-depth models over the last ~300 years
- Following the 1700 CE Cascadia Subduction Zone earthquake high marsh reestablishment took ~200 years in Netarts

Supporting Information:

Supporting Information may be found in the online version of this article.

Correspondence to:

E. K. Peck,
erinpeck@udel.edu

Citation:

Peck, E. K., Guilderson, T. P., Walczak, M. H., & Wheatcroft, R. A. (2022). Recovery rate of a salt marsh from the 1700 CE Cascadia Subduction Zone earthquake, Netarts Bay, Oregon. *Geophysical Research Letters*, *49*, e2022GL099115. https://doi.org/10.1029/2022GL099115

Received 12 APR 2022
Accepted 2 SEP 2022

Recovery Rate of a Salt Marsh From the 1700 CE Cascadia Subduction Zone Earthquake, Netarts Bay, Oregon

Erin K. Peck[1,2], Thomas P. Guilderson[3], Maureen H. Walczak[1], and Robert A. Wheatcroft[1]

[1]Earth, Ocean, & Atmospheric Sciences, Oregon State University, Corvallis, OR, USA, [2]Plant & Soil Sciences, University of Delaware, Newark, DE, USA, [3]Ocean Sciences, University of California Santa Cruz, Santa Cruz, CA, USA

Abstract Since the 1700 CE Cascadia Subduction Zone earthquake and associated coseismic subsidence and tsunami, vegetated intertidal habitats have reestablished across Pacific Northwest estuaries, yet timescales and mechanisms of recovery are uncertain. We investigated the timescale of salt marsh reestablishment in Netarts Bay, Oregon following the 1700 CE earthquake using a combination of excess ^{210}Pb, ^{14}C, stratigraphic constraints, and Bayesian age-depth modeling. Coseismic subsidence lowered the area to low/mid marsh, which persisted for 200 years before transition to modern high marsh. The modern high marsh now appears in dynamic equilibrium with modern sea level rise. In addition to serving as a methodological proof of concept for dating the past 300 years, these results provide insight into intertidal morphodynamic response to large perturbations along tectonically active margins.

Plain Language Summary The last major earthquake along the Pacific Northwest (PNW) coast occurred in 1700, causing widespread destruction of salt marshes through elevation loss and burial by tsunami sand. In the ~300 years following the earthquake, PNW salt marshes that were lost during the earthquake have reestablished; however, we are unsure of the timeframe over which they grew back. Salt marshes provide valuable services, including flood protection, habitat, pollution filtration, and carbon burial. Thus, improved understanding of their growth patterns is important—especially in response to large, destructive events such as those that will occur with increasing frequency under accelerating climate change (like hurricanes). Through a combination of different age dating techniques and statistical analyses, we determined that the reestablishment of a salt marsh in Netarts Bay, Oregon took ~200 years. Following the next major PNW earthquake, which will undoubtedly occur under accelerated sea level rise, some salt marshes and their services may be lost permanently.

1. Introduction

Cascadia Subduction Zone (CSZ) megathrust earthquakes (M_w > 8.5) are major perturbations to the Pacific Northwest (PNW) margin, producing up to 3 m of coseismic subsidence resulting in instantaneous relative sea level rise (RSLR), increased coastal accommodation space (AS), and potential deposition of sand layers by tsunami (Atwater, 1987). The most recent earthquake in 1700 CE is well preserved in Cascadia tidal wetland stratigraphic sequences (Atwater et al., 1995; Nelson et al., 1995; Peters et al., 2007). Coseismic subsidence resulted in widespread, sudden, and lasting RSLR causing many coastal environments to change elevation (e.g., high to low marsh, tidal flat to subtidal). Salt marshes that were drowned during the CSZ 1700 CE earthquake eventually reestablished, as evidenced by the extent of modern tidal wetlands, through a combination of post-seismic rebound (timing and magnitude unknown), interseismic uplift, glacial isostatic adjustment, and sediment accretion. However, it is unclear whether the pre-earthquake habitat and elevation have fully recovered, and the timeframe and mechanisms of AS filling are poorly constrained. Determining the rate of AS filling would provide insight into salt marsh morphodynamics in response to large perturbations, including non-tectonic (e.g., hurricanes, non-locally produced tsunami, spit/barrier island breaching). Moreover, elucidating the tempo of transitions between intertidal zones would improve understanding of the equilibrium timescale of the sediment routing system and thus the time-dependent trapping efficiency of the estuarine sink along a tectonically active margin (Romans et al., 2016).

Previous studies inferred minimum ages of modern PNW salt marshes (decades to ~150 years) based on historical accounts and maps (Atwater & Hemphill-Haley, 1997); Sitka spruce death (Kelsey et al., 1998) and regrowth (Benson et al., 2001); and clam bed thicknesses (Witter et al., 2003). Yet sub-century post-1700 CE AS filling

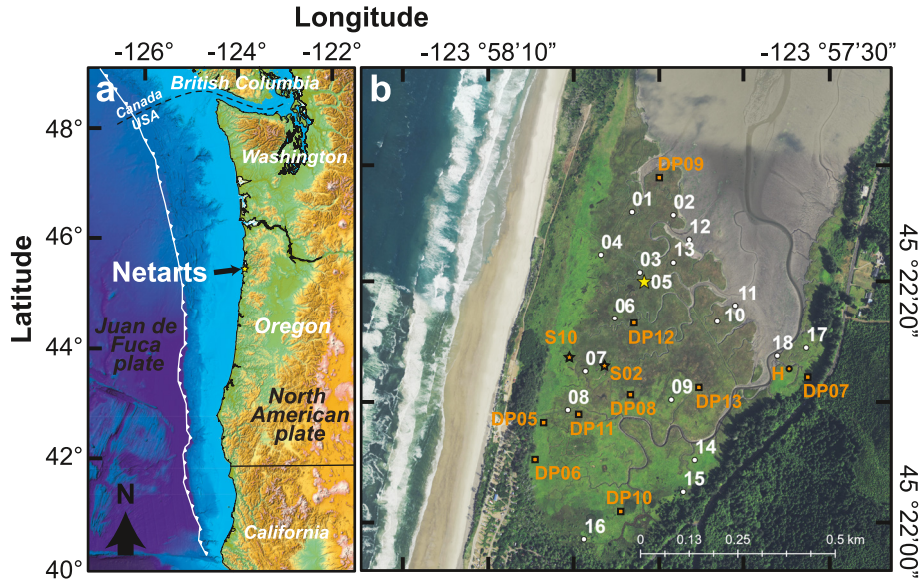

Figure 1. (a) Cascadia Subduction Zone DEM (USGS GTOPO30). (b) Netarts salt marsh (aerial image from the 2018 Oregon Statewide Imagery Program) with core locations from our study (white circles except NT05, which is labeled with a yellow star) and from Darienzo and Peterson (1990; orange square), Shennan et al. (1998; orange star), and Hawkes et al. (2005; orange circle).

rates remain elusive because no suitable dating method has been established for the last 125 to 300 years in the PNW. Excess ^{210}Pb and ^{137}Cs are appropriate for at most the last ~150 years, though ^{137}Cs may be susceptible to post-depositional mobilization (Foster et al., 2006). Lack of chronostratigraphic indicators in PNW marsh sediment and large errors associated with ^{14}C ages calibrated in this timeframe (i.e., the radiocarbon calibration curve plateau) have also hindered estimation of post-1700 CE sediment accretion rates (SARs). But, as highlighted by several studies (Blaauw et al., 2018; Ishizawa et al., 2022; Wright et al., 2017), high-density ^{14}C dating combined with Bayesian age-depth modeling may produce chronologies with decadal resolution.

We seek to answer the question: what is the timescale of salt marsh recovery following the 1700 CE megathrust earthquake? To determine the timescale of AS filling, we must first determine whether a combination of age dating techniques (excess ^{210}Pb and ^{14}C) and Bayesian age-depth modeling can produce a roughly decadal chronology for the past 300 years when analyzed with facies indicators.

2. Methods

Netarts Bay, OR (Figure 1) is a shallow (≤3 m at mean lower low tide), bar-built estuary located in a 36-km^2 watershed drained by several small creeks. At Netarts Bay, microfossil-based relative sea level reconstructions estimated coseismic subsidence during the 1700 CE earthquake as 0.4 ± 0.3 (Shennan et al., 1998), 0.26 ± 0.28 (P. L. Wang et al., 2013), and 0.38 ± 0.2 m (Kemp et al., 2018). Estimated Late Holocene RSLR (1 mm year^{-1}; Engelhart et al., 2015) is similar to modern RSLR in the region (1.5 ± 1.0 mm year^{-1}; Peck et al., 2020). Fluvial sediment input is limited (2.5 × 10^3 t year^{-1}) but present-day SARs have kept pace with RSLR (Peck et al., 2020). The salt marsh located within the southern portion of Netarts Bay was chosen to test our methods as it has a well-established stratigraphic record of CSZ earthquake/tsunami deposits, and anthropogenic alterations have been minimal.

Fifteen 2.5-m-long sediment cores collected by Peck et al. (2020; Figure 1b; Table S1 in Supporting Information S1 for coordinates and elevations; Figure S1 in Supporting Information S1 for computed tomography [CT] scans) using a push coring method had stratigraphic sequences indicative of the 1700 CE earthquake/tsunami (e.g., Shennan et al., 1998). Core NT05 (2.47-m) was chosen from possible high marsh cores for establishing a detailed chronology given its central location and particularly clear earthquake stratigraphy (Figure 2b). NT05 had a total of 10.5 cm (4%) of compaction (based on the difference in the distances to the surface inside and outside the PVC liner), similar to what others have observed (Carr et al., 2020). Within NT05, we focused on the

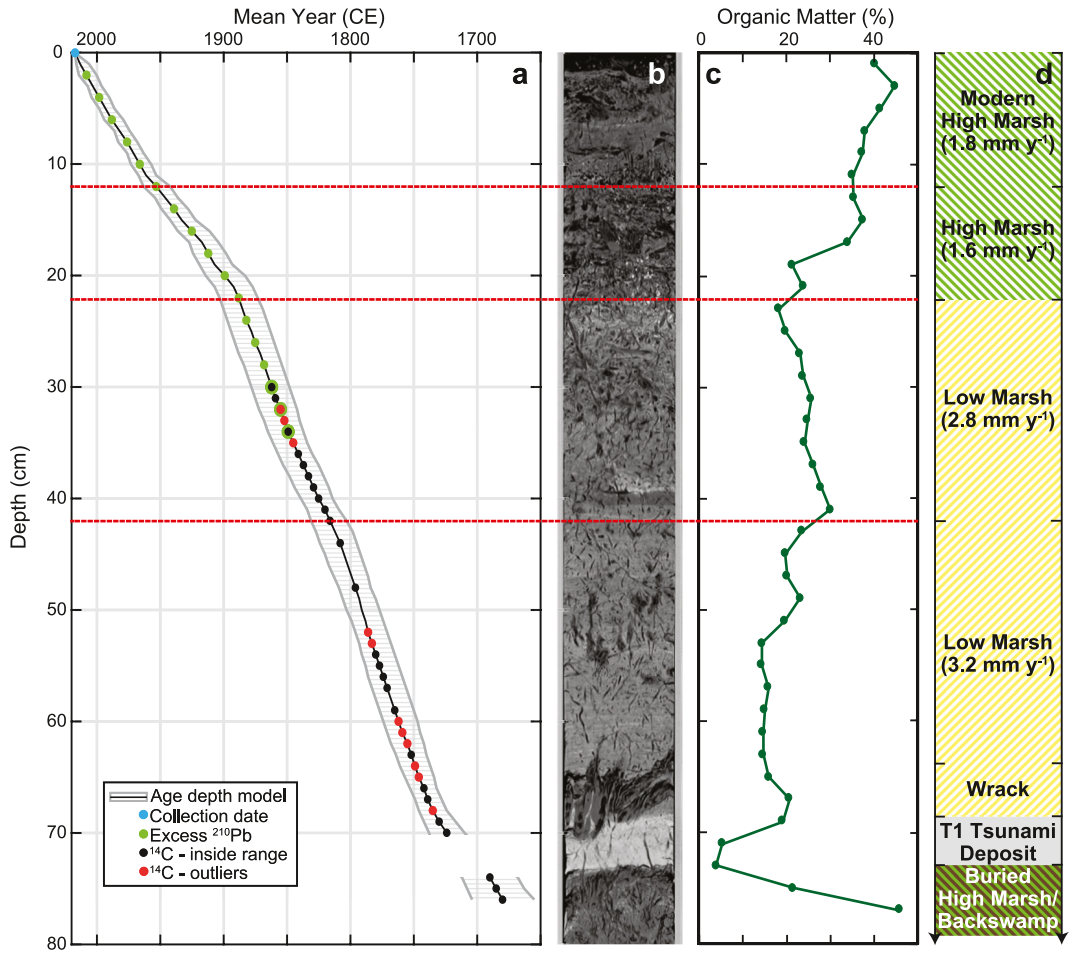

Figure 2. (a) Bacon age-depth model of NT05 with age constraints. Shaded area denotes calibrated age ranges (95% confidence). (b) X-ray CT scan of NT05. Less dense material appears darker in color and more dense material appears lighter in color. (c) Organic matter content (wt.%) with depth. Dashed red lines indicate slope breaks in the age-depth model. (d) Stratigraphic interpretation.

upper 77 cm, which extended from just below the likely 1700 CE earthquake/tsunami deposit to the modern high marsh. Excess ^{210}Pb was measured at 2-cm increments from the marsh surface/core top to analytical extinction at 34 cm by γ-ray spectroscopy (detection limit = 3 Bq kg^{-1}); ^{137}Cs was additionally measured but displayed evidence of post-depositional remobilization, so was not useful (Peck et al., 2020). The core was sampled for ^{14}C dating at 1-cm intervals from just below the earthquake/tsunami deposit at 77–29 cm, overlapping the ^{210}Pb profile. Using a stereomicroscope, terrestrial plant fragments were picked, avoiding unidentifiable materials. We preferentially searched for plant fragments that likely grew and were deposited near the sediment surface (e.g., *Potentilla* fruit and *Triglochin maritima* leaf bases and fruit/seeds), using Shennan et al. (1998) as a guide (Figure S2 and Table S2 in Supporting Information S1). 38 depths had sufficient materials for ^{14}C analysis. Abundant sample material at four depths allowed for duplicates (means were used in the age-depth model). Plant fragments and a ^{14}C-free wood background (QueetsA; Southon & Magana, 2010) were prepared using the modified de Vries (ABA) technique (de Vries & Barendsen, 1954). Samples were analyzed using either an FN (<0.6 mg; Davis et al., 1990) or Compact NEC (>0.6 mg; Broek et al., 2021) accelerator depending on weight at the Center for Accelerator Mass Spectrometry, Lawrence Livermore National Laboratory (Table S2 in Supporting Information S1). Results include a background correction and a -29 ± 2 ‰ correction was applied based on the range of δ^{13}C values for the plant fragments (Figure S2 in Supporting Information S1).

We chose Bacon (Bayesian accumulation model in R) for calibration of ^{14}C ages and creation of an age-depth model based on its seamless interface with Plum (a Bayesian model for calculating excess ^{210}Pb age-depth models that better incorporates uncertainty estimates than other excess ^{210}Pb methods; Blaauw et al., 2021) that allows

for variable SARs, and ability to ignore outliers (Aquino-López et al., 2020; Blaauw & Christen, 2011). All ^{14}C ages were included (even those above the interpreted earthquake/tsunami deposit with ranges older than 1700 CE; Table S2 in Supporting Information S1). The IntCal20 calibration curve was used (Reimer et al., 2020). Stratigraphic constraints were incorporated as model priors, including coring date and overall accumulation rate (based on depth to the 1700 CE tsunami deposit; Table S3 in Supporting Information S1 lists all Bacon/Plum inputs). The tsunami deposit was treated as an artificial hiatus between 71 and 73 cm to allow for independence between SARs above and below. To minimize the deterministic nature of Bayesian modeling, we selected a "memory" prior that indicated low dependence of SARs between neighboring depths (Blaauw & Christen, 2011). Moreover, the ^{14}C portion of the model produced by Bacon was compared to results using OxCal (Text S1 in Supporting Information S1; Bronk Ramsey, 2008; Bronk Ramsey, 2021). All presented calibrated ages are at the 95% CI. To calculate SARs over specific ranges, inflection points were identified along the Bacon/Plum age-depth model using ANCOVA (Sokal & Rohlf, 1981).

Stratigraphy in NT05 and nearby cores (Table S1 in Supporting Information S1) were assessed primarily using dry bulk density (ρ_{DB}), calculated from 1-mm-resolution X-ray CT scans (Peck et al., 2020). To estimate habitat changes, downcore NT05 ρ_{DB} was compared to ρ_{DB} in the top 10-cm of modern habitats using a Kruskal-Wallis test ($\alpha = 0.05$). Our stratigraphic paleoenvironmental interpretations are also based on organic matter (OM) content (measured by loss-on-ignition at 2-cm increments; Peck et al., 2020) and interpretation of plant fragments that had been picked for dating. Dates of habitat transitions were estimated in other modern high marsh cores based on ρ_{DB} chronologies, produced using excess ^{210}Pb analyzed by Plum (Figure S3 in Supporting Information S1).

3. Results and Discussion

3.1. Stratigraphy

Darienzo and Peterson (1990), Shennan et al. (1998), and Hawkes et al. (2005) all found litho- and bio-stratigraphic evidence of earthquakes in Netarts. Possible earthquake stratigraphy was first identified by peat layers overlain by a sharp contact with 1–10 cm sand or coarse silt that grades upward to finer-grained silt and clay. The shallowest of such sequences at Netarts were found at depths ranging from 56 to 80, 66 to 68, and 113 cm (buried peat tops; Darienzo & Peterson, 1990; Shennan et al., 1998; Hawkes et al., 2005, respectively). Further analysis of pollen, diatom, and foraminiferal/thecamoebian assemblages between the lower and upper layers surrounding the lithogenic deposit are suggestive of a CSZ earthquake when species change indicates elevation loss. Based on diatom assessment at the genus level, Darienzo and Peterson (1990) interpreted the buried peat as supratidal vegetated marsh or forested wetland with freshwater ponding and the overlying mud as low marsh (Figure 1b; sites DP5-10). Combining diatom and pollen analysis, Shennan et al. (1998) inferred high marsh or backswamp of the buried peat and low marsh of the overlying mud (Figure 1b; sites S02 and S10). Hawkes et al. (2005) assessed the area as high marsh both above and below the minerogenic deposit based on foraminiferal/thecamoebian assemblages (Figure 1b; site H). Thus, when combined with ^{14}C dates, Darienzo and Peterson (1990) and Shennan et al. (1998) interpreted the shallowest peat-mud couplet as the 1700 CE earthquake/subsidence event, while Hawkes et al. (2005) attributed a similar sequence in the eastern fringing marsh to a non-tectonic source.

Core NT05 is described here from bottom to surface. The lithology of NT05 from 77 to 74 cm is an organic-rich unit that contains abundant gas filled rhizomes (Figure 2c). A sharp contact at 74 cm in NT05 separates the buried high marsh/backswamp from a well-sorted, high ρ_{DB}, sandy deposit spanning 74–71 cm. OM content is low, with little plant material present. The sandy deposit ends in an abrupt contact above which sits a layer concentrated in rhizomes. Sediment above the buried vegetation is less OM-rich (with fewer rhizomes), denser than the sediment from 77 to 74 cm, and displays fine bedding. From 71 to 0 cm OM and rhizomes increase toward the surface, while ρ_{DB} decreases. All other high marsh cores we collected exhibit similar stratigraphy (Figure S1 in Supporting Information S1).

The lithostratigraphy of our high marsh cores is consistent with sequences described by Darienzo and Peterson (1990) and Shennan et al. (1998) at nearby sites that these authors interpreted as the 1700 CE earthquake/tsunami. The organic-rich unit from 77 to 74 cm in NT05 is most likely high marsh or scrub-shrub based on ρ_{DB} and OM content compared with surface sediments of modern marsh environments (Figure 3a), and *Potentilla* fruit between 77 and 74 cm is more indicative of high marsh in Netarts (Shennan et al., 1998). Thus, our stratigraphic assessment of plant material substantiates the interpretations of Shennan et al. (1998) that the buried

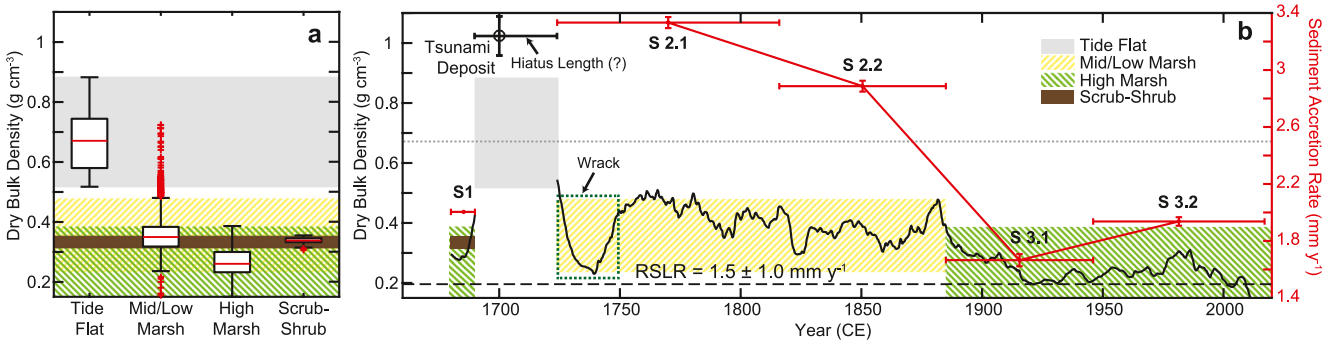

Figure 3. (a) Significantly different boxplots of ρ_{DB} measured in modern habitats (Kruskal-Wallis, df = 1,716, $p < 0.01$). (b) Dry bulk density (ρ_{DB}; black y axis) chronology in NT05 from ~1675 CE to the present. Colored boxes depict interpreted marsh zones. Mean accretion rates (red y axis) were temporally binned (duration = horizontal bars) by significant slope breaks (ANCOVA, $n = 66$, $p < 0.01$) and sections (S) are labeled. Twentieth century relative sea level rise and uncertainty (1.5 ± 1 mm year^{-1}), consistent with the Late Holocene rate, are represented by black dashed and gray dotted lines, respectively.

marsh at NT05 was high marsh/backswamp. The shallowest (~70–60 cm) lithogenic layers in our high marsh cores are similar in lithology and depth to those previously dated to 1700 CE (Darienzo & Peterson, 1990; Shennan et al., 1998). Further, the plant material above the tsunami deposit in NT05 may be wrack as rhizomes are less abundant in overlying sediment (wrack is less evident in other cores, though it has been observed in previous earthquake/subsidence deposits by Darienzo & Peterson, 1990). Sediment immediately overlying the 1700 CE tsunami deposit is interpreted as low marsh based on ρ_{DB} and OM content (Figure 3), consistent with the biostratigraphic analysis of Darienzo and Peterson (1990) and Shennan et al. (1998). NT05 stratigraphy returns to high marsh based on ρ_{DB}, OM content, modern vegetation assemblages, and elevation; the depth/timing of the low to high marsh transition is discussed below.

3.2. Age-Depth Relationship

Calibrated and modeled ^{14}C ages from NT05 extended from 1680 cal CE ± 25 years at 76 cm to 1862 cal CE ± 15 years at 30 cm with a mean uncertainty of ±13 years (range = ±0–25 years; Figure 2a; Table S4 in Supporting Information S1). Modeled excess ^{210}Pb ages from NT05 extended from 1849 cal CE ± 14 years at 34 cm to 2017 CE at 0 cm (the date of collection) with a mean uncertainty of ±12 years (max = 16 years). Mean calibrated ages were well centered in their ranges, deviating by <5 years. Our results indicate that ^{14}C dating at 1-cm intervals can produce a roughly decadal chronology when combined with independently estimated dates (e.g., excess ^{210}Pb) and detailed stratigraphic knowledge (ours and others; Darienzo & Peterson, 1990; Hawkes et al., 2005; Shennan et al., 1998). Within the ^{14}C dated depth horizons, the Bacon age-depth model was almost identical to that produced by OxCal (Figure S4 in Supporting Information S1). Dates calibrated and modeled using OxCal were 1–22 years (mean = 8 ± 6 years) different from those of Bacon. In a comparison of different, commonly used Bayesian age-depth models, Wright et al. (2017) noted that Bacon tends to produce a temporal offset (i.e., modeled age-depth model leads the true curve though the pattern is generally correct); however, the effect typically occurred when analyzing larger sediment sample interval thicknesses. Our use of 1-cm-thick layers when possible and stratigraphic constraints likely averted a temporal offset effect. Although these results are promising, statistical methods cannot overcome potential methodological shortcomings, if they exist, so we assess potential sources of error below.

Disturbance to the sediment profile, particularly compaction, is common in stratigraphic studies using cores (Carr et al., 2020). Comparison between measured and modeled ρ_{DB}, based on the downcore OM (Figure S5 in Supporting Information S1; Bird et al., 2004), indicates that the 10.5 cm of compaction is relatively uniform over the top 70 cm. Incorporation of compaction only raises the bulk SAR estimate by 0.3 mm year^{-1} 1700–2017 CE; thus, compaction is not a major source of error to the overall interpretation.

The QueetsA wood yielded a ^{14}C age of 51,760 ± 200 years, consistent with other analyses (Southon & Magana, 2010). Three of four duplicates returned ^{14}C ages that were not significantly different (Table S2 in Supporting Information S1), indicating good agreement at each depth. The depth with significantly different duplicate dates (39 cm) indicates there may be other outliers, and indeed, a few ^{14}C ages were anomalously old

(Table S2 in Supporting Information S1). Even though we focused our dating efforts on short-lived, salt marsh plant parts, some anomalously old dates are expected given the possibility of a landscape residence time or incorporation of reworked sediment with older plant material, as others have observed, especially with high-density dating (Gedye, 1998; Kilian et al., 1995). Yet, despite some anomalously old ^{14}C ages, the calibrated age-depth model falls within the expected age range because Bacon is optimized through the use of a Student's *t*-distribution to ignore outlying data (Blaauw & Christen, 2011). OxCal, when outliers are removed, produces a similar age-depth model (Figure S4 in Supporting Information S1).

We assess the accuracy of the age-depth model within the context of probable salt marsh morphodynamic responses following the 1700 CE earthquake subsidence and tsunami. As an example, the age-depth model indicates a depositional hiatus occurred following the tsunami (71 cm) lasting 10–38 years; however, a prolonged hiatus is unlikely in a vegetated salt marsh with recently created AS. A hiatus is especially unlikely in Netarts, where coseismic subsidence only converted high to low marsh, rather than higher energy tidal flat or subtidal elevations. Given that the duplicate dates measured between 71 and 70 cm (just above the subsidence contact) were in close agreement and are likely not reworked (as the age range skews too young), it is quite probable that the models (both Bacon and OxCal) estimated this age too young. Indeed, the calibrated ^{14}C age distribution extends older than 1700 CE. An older age at 71–70 cm would have produced a faster SAR in the three decades following the 1700 CE earthquake. Thus, despite specifying a low dependence of SARs between neighboring depths, both Bayesian models tend to favor constant SAR chronologies. We therefore focus interpretations on general patterns in SARs rather than analyzing differences between individual ages/depths.

Overall, the combination of ^{14}C measured at high sampling density with Bayesian modeling can produce a robust decadal chronology for the last ~300 years, but the likelihood of success is greatest when the study area has independent age constraints via other radiometric age dates (e.g., excess ^{210}Pb, ^{137}Cs) and/or a well-defined event stratigraphy (e.g., tsunami, floods, wildfire, tephras, varves, pollen). Thus, the methods outlined herein could be applied elsewhere, in active (e.g., across the CSZ, Alaska, New Zealand, Chile) or passive settings, for the last 300 years. The desired age resolution can be achieved by multiplication with an estimated bulk SAR to determine appropriate sampling intervals (e.g., 0.2 cm year^{-1} SAR × 5 years resolution = 1 cm sampling). Further, a modification of the outlined method could be applied during periods when the ^{14}C calibration curve plateaus by combining high-depth-resolution ^{14}C measurements with other dating techniques like those listed above.

3.3. Accretion History and Habitat Change

The age-depth model over the last ~300 years can be subdivided into three major sections based on statistically different slopes (ANCOVA, $n = 66$, $p < 0.01$; Figure 3b; Figure 2d).

3.3.1. Buried High Marsh (77–74 cm; 1680 cal CE ± 25 Years 1700 CE)

Prior to the 1700 CE earthquake, the buried high marsh/backswamp SAR (2.0 ± 0.0 mm year^{-1}; Figure 3b) suggests that the system was in dynamic equilibrium with RSLR, which is a typical feature of high marsh elevations (Kirwan et al., 2016), for at least two decades. Moreover, as previously outlined, Netarts salt marsh was interpreted high marsh or backswamp based on diatom and pollen analysis by Shennan et al. (1998) and the fringing marsh to the west was assessed as high marsh by Hawkes et al. (2005). Heterogeneity in habitat types across the marsh is expected, and areas to the south and along the marsh-upland perimeter may have been scrub-shrub or forested wetland prior to the 1700 CE earthquake/tsunami as determined by Darienzo and Peterson (1990), which would be similar to modern habitat extents.

3.3.2. Low/Mid Marsh (71–23 cm; 1724 cal CE ± 14 Years to 1885 cal CE ± 16 Years)

Following the 1700 CE earthquake, the low/mid marsh persisted for 200 years during which time SARs (mean = 3.0 ± 0.02 mm year^{-1}) were greater than rates currently observed in the modern marsh (1.9 ± 0.6 mm year^{-1}, $n = 14$; Peck et al., 2020), a typical feature of low marsh elevations (Kirwan et al., 2016). Our facies reconstruction agrees well with the biostratigraphic assessments of others who found that sediment overlying the 1700 CE subsidence contact and tsunami sand contains diatom, pollen, and foraminifera assemblages indicative of low marsh (Darienzo & Peterson, 1990; Shennan et al., 1998). The 200 year persistence of low marsh indicates that, while the timing, magnitude, and sign of post-seismic motion is poorly constrained in Netarts, there was at least not an equivalent rebound to coseismic subsidence as high marsh might have otherwise

reestablished immediately. SARs slowed around 1816 cal CE ± 14 years (42 cm) but based on ρ_{DB} the system likely remained low/mid marsh until 1885 cal CE ± 16 years (Figure 3). Elevated SARs in the century following the 1700 CE earthquake could have resulted from a combination of factors. First, increased AS lengthens hydroperiod, resulting in longer periods of sediment settling. Further, greater sediment loads may be expected if the 1700 CE destabilized slopes, causing landslides (Richardson et al., 2018). Deepening of the subtidal environment associated with earthquake subsidence could have also increased water velocities, resuspending and redistributing sediment in the bay. A relative slowing of SARs from 1816 cal CE ± 14 years to 1885 cal CE ± 16 years as the marsh gained elevation likely occurred as hydroperiods shortened, thereby reducing tidal inundation depths and ultimately the amount of sediment settling.

3.3.3. Modern High Marsh (23–0 cm; 1885 cal CE ± 16 Years to 2017 CE)

The transition from low/mid to high marsh occurred at 1885 cal CE ± 16 years, resulting in a significant decrease in SARs and ρ_{DB} more akin to present high marsh (Figure 3). SARs over the last 130 years are comparable to the modern RSLR rate (1.5 ± 1.0 mm year^{-1}), indicating that the system reached a dynamic equilibrium (Redfield, 1972). Nearby cores transitioned from low/mid to high marsh at around the same time as NT05, between 1875 cal CE ± 39 years and 1909 cal CE ± 20 years (Table S1 and Figure S6 in Supporting Information S1). Thus, reestablishment of much of the Netarts salt marsh to the pre-1700 CE conditions took ~200 years.

3.3.4. Reestablishment and Implications

Why did AS filling following the 1700 CE earthquake take two centuries in Netarts salt marsh despite previous estimates in other CSZ marshes of decades to ~150 years (Atwater & Hemphill-Haley, 1997; Benson et al., 2001; Kelsey et al., 1998; Witter et al., 2003)? Variation in reestablishment rates may be due to methodological differences between previous workers and our own; however, two centuries for reestablishment in Netarts was particularly surprising given relatively limited coseismic subsidence compared to other CSZ marshes. The timing of reestablishment of the Netarts high marsh could have been limited compared to other CSZ basins by its small watershed and thus meager fluvial sediment loads that possibly starved the marsh of sediment necessary for accretion. Given the current marsh extent and mean SARs, only ~35% of fluvial sediment is trapped annually (Peck et al., 2020); however, faster accretion and progradation of the marsh during reestablishment would require higher sediment trapping. Moreover, sediment delivery to the platform may be hampered under a restricted tidal prism following the earthquake if the tsunami infilled subtidal portions of the relatively shallow bay. The near extirpation of beaver (*Castor canadensis*) on the PNW coast since the 1800s (Diefenderfer & Montgomery, 2009) may also relate to the slowing of SARs in 1816 cal CE ± 14 years, resulting in an additional century before high marsh recovery. Beaver dams help slow inundating water, increasing sediment settling over the marsh, although presumably a similar trend in SARs would be observed elsewhere as beaver trapping was ubiquitous amongst CSZ watersheds/estuaries. Ultimately, to better assess salt marsh response along the entire CSZ, age-depth modeling technique outlined here should be applied along elevation transects in systems with ranges in terms of coseismic subsidence, interseismic RSLR, suspended sediment supply, tidal range, and anthropogenic influence.

In our methodological proof of concept, we provide insights into an understudied process—salt marsh morphodynamic response to subduction zone earthquakes—along an important portion of the North American coastline. Understanding the timescale of salt marsh recovery is critical to predicting the fate of CSZ coastal habitats and their ecosystem services following the next major earthquake, which will undoubtedly occur under accelerated RSLR. Furthermore, the 200 year-long recovery of the Netarts salt marsh despite limited coseismic subsidence highlights the need to determine drivers of AS filling, applicable to other intertidal zones globally that are responding to perturbation events, tectonic or otherwise. Additionally, tracking the propagation of large, episodic events within sediment routing systems helps inform the completeness of the sediment record, critical to assessing recurrence intervals (Benson et al., 2001). Further, the outlined dating technique could help identify (or shed doubt on) 1700 CE stratigraphy along the Cascadia margin in coastal marshes, lakes, and offshore sediments, particularly important given uncertainty surrounding the extent of the rupture (Melgar, 2021). A detailed assessment of post-1700 CE SARs along the entire CSZ may also provide insight into thresholds for the creation and preservation of earthquake/tsunami deposits in marsh stratigraphy (Nelson et al., 2021), as well as inform estimates of post-seismic and interseismic deformation. For instance, application of the outlined methods could help substantiate or challenge timeframes and magnitudes of modeled elastic rebound (K. Wang, 2007). Clearly further investigation is needed, but we have provided evidence that decadal age-depth modeling is possible and one tool by which we can address pressing questions related to salt marsh morphodynamics.

Conflict of Interest

The authors declare no conflicts of interest relevant to this study.

Data Availability Statement

^{210}Pb activities and ρ_{DB} data are available at https://doi.org/10.25573/serc.11317820.

Acknowledgments
Netarts is the traditional homelands of the Tillamook, Siletz, and Nestucca. Descendants are part of the Confederated Tribes of Grand Ronde Community of Oregon and Confederated Tribes of the Siletz Indians. Thoughtful, thorough suggestions provided by journal reviewers greatly improved the quality of our manuscript. We thank B. Buchholz for assistance with ^{14}C analyses, and L. Brophy and M. Goñi for comments on earlier drafts. We received funding from Geological Society of America Awards for Geochronology Student Research and Oregon Sea Grant.

References

Aquino-López, M. A., Ruiz-Fernández, A. C., Blaauw, M., & Sanchez-Cabeza, J. A. (2020). Comparing classical and Bayesian ^{210}Pb dating models in human-impacted aquatic environments. *Quaternary Geochronology*, *60*, 101106. https://doi.org/10.1016/j.quageo.2020.101106

Atwater, B. F. (1987). Evidence for great Holocene earthquakes along the outer coast of Washington State. *Science*, *236*(4082), 942–944. https://doi.org/10.1126/science.236.4804.942

Atwater, B. F., & Hemphill-Haley, E. (1997). *Recurrence intervals for great earthquakes of the past 3,500 years at northeastern Willapa Bay, Washington. (Professional Paper 1576, 108 p.)*. U.S. Geological Survey. https://doi.org/10.3133/pp1576

Atwater, B. F., Nelson, A. R., Clague, J. J., Carver, G. A., Yamaguchi, D. K., Bobrowsky, P. T., et al. (1995). Summary of coastal geologic evidence for past great earthquakes at the Cascadia subduction zone. *Earthquake Spectra*, *11*(1), 1–18. https://doi.org/10.1193/1.1585800

Benson, B. E., Atwater, B. F., Yamaguchi, D. K., Amidon, L. J., Brown, S. L., & Lewis, R. C. (2001). Renewal of tidal forests in Washington State after a subduction earthquake in AD 1700. *Quaternary Research*, *56*(2), 139–147. https://doi.org/10.1006/qres.2001.2251

Bird, M. I., Fifield, L. K., Chua, S., & Goh, B. (2004). Calculating sediment compaction for radiocarbon dating of intertidal sediments. *Radiocarbon*, *46*(1), 421–435. https://doi.org/10.1017/S0033822200039734

Blaauw, M., & Christen, J. A. (2011). Flexible paleoclimate age-depth models using an autoregressive gamma process. *Bayesian Analysis*, *6*(3), 457–474. https://doi.org/10.1214/11-BA618

Blaauw, M., Christen, J. A., Aqunio-Lopex, M. A., Esquivel-Vazquez, J., Gonzalez, V. O. M., Belding, T., et al. (2021). rplum (version 0.2.2) [Software]. Retrieved from https://cran.r-project.org/web/packages/rplum/rplum.pdf .

Blaauw, M., Christen, J. A., Bennett, K. D., & Reimer, P. J. (2018). Double the dates and go for Bayes—Impacts of model choice, dating density and quality on chronologies. *Quaternary Science Reviews*, *188*, 58–66. https://doi.org/10.1016/j.quascirev.2018.03.032

Broek, T. A., Ognibene, T. J., McFarlane, K. J., Moreland, K. C., Brown, T. A., & Bench, G. (2021). Conversion of the LLNL/CAMS 1 MV biomedical AMS system to a semi-automated natural abundance ^{14}C spectrometer: System optimization and performance evaluation. *Nuclear Instruments and Methods in Physics Research Section B: Beam Interactions with Materials and Atoms*, *499*, 124–132. https://doi.org/10.1016/j.nimb.2021.01.022

Bronk Ramsey, C. (2008). Deposition models for chronological records. *Quaternary Science Reviews*, *27*(1–2), 42–60. https://doi.org/10.1016/j.quascirev.2007.01.019

Bronk Ramsey, C. (2021). OxCal (version 4.4.4) [Software]. Retrieved from https://c14.arch.ox.ac.uk/oxcal.html .

Carr, S. J., Diggens, L. M., & Spencer, K. L. (2020). There is no such thing as "undisturbed" soil and sediment sampling: Sampler-induced deformation of salt marsh sediments revealed by 3D X-ray computed tomography. *Journal of Soils and Sediments*, *20*(7), 2960–2976. https://doi.org/10.1007/s11368-020-02655-7

Darienzo, M. E., & Peterson, C. D. (1990). Episodic tectonic subsidence of late Holocene salt marshes, northern Oregon central Cascadia margin. *Tectonics*, *9*(1), 1–22. https://doi.org/10.1029/TC009i001p00001

Davis, J. C., Proctor, I. D., Southon, J. R., Caffee, M. W., Heikkienen, D. W., Roberts, M. L., et al. (1990). LLNL/UC AMS facility and research program. *Nuclear Instruments and Methods in Physics Research Section B: Beam Interactions with Materials and Atoms*, *52*(3–4), 269–272. https://doi.org/10.1016/0168-583X(90)90419-U

de Vries, H. L., & Barendsen, G. W. (1954). Measurements of age by the carbon-14 technique. *Nature*, *174*(4442), 1138–1141. https://doi.org/10.1038/1741138a0

Diefenderfer, H. L., & Montgomery, D. R. (2009). Pool spacing, channel morphology, and the restoration of tidal forested wetlands of the Columbia River, USA. *Restoration Ecology*, *17*(1), 158–168. https://doi.org/10.1111/j.1526-100X.2008.00449.x

Engelhart, S. E., Vacchi, M., Horton, B. P., Nelson, A. R., & Kopp, R. E. (2015). A sea-level database for the Pacific coast of central North America. *Quaternary Science Reviews*, *113*(1), 78–92. https://doi.org/10.1016/j.quascirev.2014.12.001

Foster, I. D., Mighall, T. M., Proffitt, H., Walling, D. E., & Owens, P. N. (2006). Post-depositional ^{137}Cs mobility in the sediments of three shallow coastal lagoons, SW England. *Journal of Paleolimnology*, *35*(4), 881–895. https://doi.org/10.1007/s10933-005-6187-6

Gedye, S. J. (1998). *Mass balance in recent peats (doctoral dissertation). ProQuest dissertations express*. Retrieved from https://dissexpress.umi.com/dxweb/search.html. University of Liverpool.

Hawkes, A. D., Scott, D. B., Lipps, J. H., & Combellick, R. (2005). Evidence for possible precursor events of megathrust earthquakes on the west coast of North America. *The Geological Society of America Bulletin*, *117*(7–8), 996–1008. https://doi.org/10.1130/B25455.1

Ishizawa, T., Goto, K., Nishimura, Y., Miyairi, Y., Sawada, C., & Yokoyama, Y. (2022). Paleotsunami history along the northern Japan trench based on sequential dating of the continuous geological record potentially inundated only by large tsunamis. *Quaternary Science Reviews*, *279*, 107381. https://doi.org/10.1016/j.quascirev.2022.107381

Kelsey, H. M., Witter, R. C., & Hemphill-Haley, E. (1998). Response of a small Oregon estuary to coseismic subsidence and postseismic uplift in the past 300 years. *Geology*, *26*(3), 231–234. https://doi.org/10.1130/0091-7613

Kemp, A. C., Cahill, N., Engelhart, S. E., Hawkes, A. D., & Wang, K. (2018). Revising estimates of spatially variable subsidence during the AD 1700 Cascadia earthquake using a Bayesian foraminiferal transfer function. *Bulletin of the Seismological Society of America*, *108*(2), 654–673. https://doi.org/10.1785/0120170269

Kilian, M. R., Van der Plicht, J., & Van Geel, B. (1995). Dating raised bogs: New aspects of AMS 14C wiggle matching, a reservoir effect and climatic change. *Quaternary Science Reviews*, *14*(10), 959–966. https://doi.org/10.1016/0277-3791(95)00081-X

Kirwan, M. L., Temmerman, S., Skeehan, E. E., Guntenspergen, G. R., & Fagherazzi, S. (2016). Overestimation of marsh vulnerability to sea level rise. *Nature Climate Change*, *6*(3), 253–260. https://doi.org/10.1038/nclimate2909

Melgar, D. (2021). Was the January 26th, 1700 Cascadia earthquake part of a rupture sequence? *Journal of Geophysical Research: Solid Earth*, *126*(10), e2021JB021822. https://doi.org/10.1029/2021JB021822

Nelson, A. R., Atwater, B. F., Bobrowsky, P. T., Bradley, L. A., Clague, J. J., Carver, G. A., et al. (1995). Radiocarbon evidence for extensive plate-boundary rupture about 300 years ago at the Cascadia subduction zone. *Nature*, *378*(6555), 371–374. https://doi.org/10.1038/378371a0

Nelson, A. R., DuRoss, C. B., Witter, R. C., Kelsey, H. M., Engelhart, S. E., Mahan, S. A., et al. (2021). A maximum rupture model for the central and southern Cascadia subduction zone—Reassessing ages for coastal evidence of megathrust earthquakes and tsunamis. *Quaternary Science Reviews*, *261*(1), 106922. https://doi.org/10.1016/j.quascirev.2021.106922

Peck, E. K., Wheatcroft, R. A., & Brophy, L. S. (2020). Controls on sediment accretion and blue carbon burial in tidal saline wetlands. Insights from the Oregon coast, USA. *Journal of Geophysical Research: Biogeosciences*, *125*(2), e2019JG005464. https://doi.org/10.1029/2019JG005464

Peters, R., Jaffe, B., & Gelfenbaum, G. (2007). Distribution and sedimentary characteristics of tsunami deposits along the Cascadia margin of Western North America. *Sedimentary Geology*, *200*(3–4), 372–386. https://doi.org/10.1016/j.sedgeo.2007.01.015

Redfield, A. C. (1972). Development of a New England salt marsh. *Ecological Monographs*, *42*(2), 201–237. https://doi.org/10.2307/1942263

Reimer, P. J., Austin, W. E., Bard, E., Bayliss, A., Blackwell, P. G., Ramsey, C. B., et al. (2020). The IntCal20 Northern Hemisphere radiocarbon age calibration curve (0–55 cal kBP). *Radiocarbon*, *62*(4), 725–757. https://doi.org/10.1017/RDC.2020.41

Richardson, K. N. D., Hatten, J. A., & Wheatcroft, R. A. (2018). 1500 years of lake sedimentation due to fire, earthquakes, floods and land clearance in the Oregon Coast Range: Geomorphic sensitivity to floods during timber harvest period. *Earth Surface Processes and Landforms*, *43*(7), 1496–1517. https://doi.org/10.1002/esp.4335

Romans, B. W., Castelltort, S., Covault, J. A., Fildani, A., & Walsh, J. P. (2016). Environmental signal propagation in sedimentary systems across timescales. *Earth-Science Reviews*, *153*, 7–29. https://doi.org/10.1016/j.earscirev.2015.07.012

Shennan, I., Long, A. J., Rutherford, M. M., Innes, J. B., Green, F. M., & Walker, K. J. (1998). Tidal marsh stratigraphy, sea-level change and large earthquakes—II: Submergence events during the last 3500 years at Netarts Bay, Oregon, USA. *Quaternary Science Reviews*, *17*(4–5), 365–393. https://doi.org/10.1016/S0277-3791(97)00055-3

Sokal, R. R., & Rohlf, F. J. (1981). *Biometry* (2nd ed.). W.H. Freeman and Company.

Southon, J. R., & Magana, A. L. (2010). A comparison of cellulose extraction and ABA pretreatment methods for AMS ^{14}C dating of ancient wood. *Radiocarbon*, *52*(3), 1371–1379. https://doi.org/10.1017/S0033822200046452

Wang, K. (2007). Elastic and viscoelastic models of subduction earthquake cycles, In T. H. Dixon & J. C. Moore (eds.) *The seismogenic zone of subduction thrust faults* (pp. 540–575). Columbia University Press.

Wang, P. L., Engelhart, S. E., Wang, K., Hawkes, A. D., Horton, B. P., Nelson, A. R., & Witter, R. C. (2013). Heterogeneous rupture in the great Cascadia earthquake of 1700 inferred from coastal subsidence estimates. *Journal of Geophysical Research: Solid Earth*, *118*(5), 2460–2473. https://doi.org/10.1002/jgrb.50101

Witter, R. C., Kelsey, H. M., & Hemphill-Haley, E. (2003). Great Cascadia earthquakes and tsunamis of the past 6700 years, Coquille River estuary, southern coastal oregon. *The Geological Society of America Bulletin*, *115*(10), 1289–1306. https://doi.org/10.1130/B25189.1

Wright, A. J., Edwards, R. J., van de Plassche, O., Blaauw, M., Parnell, A. C., van der Borg, K., et al. (2017). Reconstructing the accumulation history of a saltmarsh sediment core: Which age-depth model is best? *Quaternary Geochronology*, *39*, 35–67. https://doi.org/10.1016/sj.quageo.2017.02.004

References From the Supporting Information

Engelhart, S. E., Horton, B. P., Vane, C. H., Nelson, A. R., Witter, R. C., Brody, S. R., & Hawkes, A. D. (2013). Modern foraminifera, δ^{13}C, and bulk geochemistry of central Oregon tidal marshes and their application in paleoseismology. *Palaeogeography, Palaeoclimatology, Palaeoecology*, *377*(1), 13–27. https://doi.org/10.1016/j.palaeo.2013.02.032

Guy, R. D., Reid, D. M., & Krouse, H. R. (1986). Factors affecting ^{13}C/^{12}C ratios of inland halophytes. II. Ecophysiological interpretations of patterns in the field. *Canadian Journal of Botany*, *64*(11), 2700–2707. https://doi.org/10.1139/b86-356

Morris, J. T., Barber, D. C., Callaway, J. C., Chambers, R., Hagen, S. C., Hopkinson, C. S., et al. (2016). Contributions of organic and inorganic matter to sediment volume and accretion in tidal wetlands at steady state. *Earth's Future*, *4*(4), 110–121. https://doi.org/10.1002/2015EF000334

Silim, S., Guy, R., Patterson, T., & Livingston, N. (2001). Plasticity in water-use efficiency of *Picea sitchensis*, *P. glauca* and their natural hybrids. *Oecologia*, *128*(3), 317–325. https://doi.org/10.1007/s004420100659